Impact of Geometry on the TM Photonic Band Gaps of Photonic Crystals and Quasicrystals

Lin Jia,[1] Ion Bita,[2] and Edwin L. Thomas[1,*]

[1]*Institute for Soldier Nanotechnologies, Department of Materials Science and Engineering, Massachusetts Institute of Technology, Cambridge, Massachusetts 02139, USA*

[2]*Qualcomm MEMS Technologies, San Jose, California 95134, USA*

(Received 1 August 2011; published 2 November 2011)

Here we demonstrate a novel quantitative procedure to pursue statistical studies on the geometric properties of photonic crystals and photonic quasicrystals (PQCs) which consist of separate dielectric particles. The geometric properties are quantified and correlated to the size of the photonic band gap (PBG) for wide permittivity range using three characteristic parameters: shape anisotropy, size distribution, and feature-feature distribution. Our concept brings statistical analysis to the photonic crystal research and offers the possibility to predict the PBG from a morphological analysis.

DOI: 10.1103/PhysRevLett.107.193901 PACS numbers: 42.70.Qs, 02.60.−x, 78.20.Bh, 78.67.Pt

One of the major recent revolutions in photonics, the photonic crystal, was proposed in 1987 [1]. Two-dimensional (2D) photonic crystals are core components in a wide range of photonic applications [2–7], for example, optical circuits, spontaneous emission control devices, quantum information devices, waveguides, lasers, nonlinear interactions, and optical communications. All the above applications are enabled by the PBG, which determines the device quality and working frequency. Topology optimization procedures for photonic crystals [8] and PQCs [9] have been developed to achieve premier PBG properties. However, the physical meanings behind the numerical optimization procedures have not been revealed and the detailed role of the particular geometric factors on determining the PBG size has not yet been clearly identified.

In this Letter, we demonstrate a statistical analysis on the geometric properties of 2D photonic structures. Three geometric parameters (shape anisotropy parameter, size distribution parameter, and feature to feature distance distribution parameter) are identified to have strong correlation with the associated PBGs.

Five periodic photonic crystals [Figs. 1(a) through 1(e)] and 12 PQCs [Figs. 1(f) through 1(q)], all with the same filling ratio ($f = 0.18$), are analyzed. This particular filling ratio is selected in order for those structures to have large transverse magnetic (TM) PBGs. The structures are chosen to cover a wide range of morphologies and rotational symmetries (two, four, six, eight, ten, and, 12-fold) to effectively represent the various types of 2D PBG structures. Structures in Fig. 1(a) through 1(e) are made by placing rods on a periodic lattice. The characteristic length scale d_0 is the lattice constant. Structures in Fig. 1(f) through 1(k) are made by placing rods or ovals on the vertices of the eightfold, tenfold, and 12-fold quasicrystal tilings generated by projection into two dimensions from a higher dimensional space. The characteristic scale d_0 is the distance between the central particle at rotational symmetric axis and its neighbor particles. PQCs in Fig. 1(l) through 1(q) are defined by the following level set equation [10,11]:

$$f(x, y) = \sum_{n=0}^{N-1} \cos[2\pi x \cos(\pi n/N)/d_0 + 2\pi y \sin(\pi n/N)/d_0 + \varphi]. \quad (1)$$

Here $f(x, y)$ is a numerical landscape in the 2D plane which assigns a value to the general point with coordinate (x, y). In Eq. (1), d_0 is the characteristic length scale of the PQCs. If $f(x, y) > t$, position (x, y) is occupied by material; if $f(x, y) < t$, position (x, y) is occupied by air. Here t is a parameter which can be tuned to change the filling ratio of the resultant structure. The PQCs have Fourier transform patterns with $2N$-fold rotational symmetry.

A large TM PBG is usually found in 2D structures consisting of separate dielectric particles and it is recognized that the particle resonances, which correspond to the peaks of the scattering cross section (SCS) [12], lead to the formation of the TM PBG [12–17]. If the optical wave frequency is slightly higher than the first resonance frequency of the particle, the transmitted wave passing through the particles is antiphase with the incoming wave, which leads to destructive interference and the reflectance of the incoming optical wave [12]. Resonance is believed to be the main physical reason for the formation of the TM PBGs for frequencies falling between the first and second resonance frequencies [12]. Such TM PBGs are rather insensitive to the positional disorder of the particles [13,14].

Next, we provide a statistical analysis on the features of the PBG structures shown in Fig. 1 and select three important geometric parameters which strongly influence the corresponding TM PBG. The first parameter is the shape anisotropy parameter (α). The particle shape brings strong impact on the scattering properties; therefore it is highly related to the TM PBG. For a typical noncircular particle, we can define the averaged radius: $\bar{r} = \sqrt{A/\pi}$, here A is the area of the particle. For an arbitrary point on the surface of

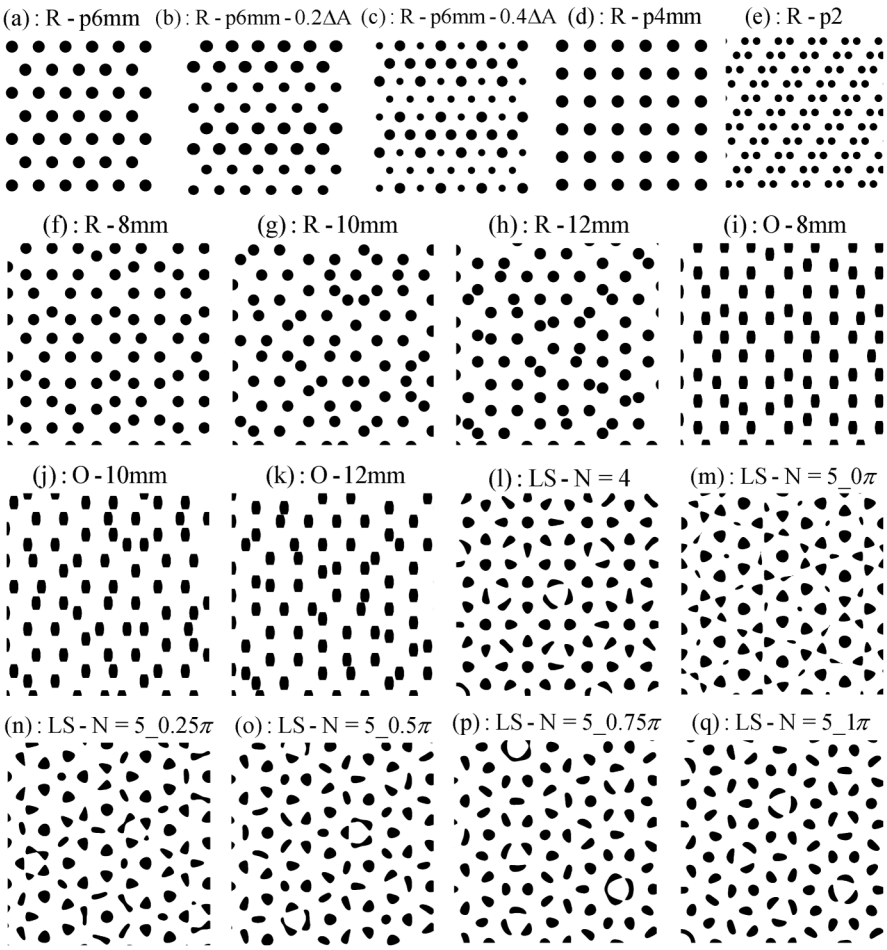

FIG. 1. The 17 photonic structures examined. The structure index is shown above each figure. Here R stands for rods; O stands for oval; LS stands for level set equations and the rotational symmetry of the associated PQC is $2N$. (a): rods in a triangular lattice; (b) rods in a triangular lattice, the rods have two area values: 1.2 and 0.8 A; (c) rods in a triangular lattice, the rods have two area values: 1.4 and 0.6 A; (d) rods in a square lattice; (e) rods in a parallelogram lattice; (f) through (h): QCs from placing rods in 8 mm, 10 mm, 12 mm QC tilings; (i) through (k): QCs from placing ovals in 8 mm, 10 mm, 12 mm QC tilings; (l) through (q) QCs from level set equations. The value in the end of the structural index (0π, 0.25π, 0.5π, 0.75π, or 1π) stands for phase value φ in Eq. (1). For $N = 4$, all φ values lead to the same structure; therefore, there is no φ value at the end of the structural index.

the particle, $\vec{r}$ denotes the vector from the center of mass to the surface point. $\Delta r = |\vec{r}| - \bar{r}$ indicates the deviation of the particle shape from the isotropic circular shape. For circular shape particle, Δr equals zero at all surface points. The normalized integration of Δr over the particle i is

$$Q = \sqrt{\oint_{\partial S} \Delta r_i^2 ds}/S_i \bar{r}_i. \tag{2}$$

Here, S_i is the perimeter of the particle i and ∂S is the particle surface. The shape anisotropy factor α is defined by the averaged Q for the PBG structure

$$\alpha = \sum_{i=1}^{M} \left(\sqrt{\oint_{\partial s} \Delta r_i^2 ds}/S_i \bar{r}_i \right)/M. \tag{3}$$

Here, M is the total number of particles. For the structures investigated, we choose a fundamental domain with $M \sim 1000$; $\sum_{i=1}^{M}$ is the sum for all M particles. The larger the α parameter, the more the particle shape deviates from the circular shape. A noncircular dielectric feature has different scattering cross section for waves incident from different angles, which is disadvantageous to achieve wave propagation suppression for all in-plane directions; therefore a larger value of α leads to a lower TM PBG consistent with the observation that the structures comprised of circular elements are found to open larger TM PBGs than the structures consisting of noncircular elements [9,18].

The size of the particle determines the resonance frequency ($f \propto 1/r$). The second structural characterization factor β is the standard deviation of the areas of the particles:

$$\beta = \sqrt{\sum_{i=1}^{M} (A_i - \bar{A})^2/(M-1)}/\bar{A}. \tag{4}$$

Here, $\bar{A}$ is the averaged area of the M particles. A larger β indicates a more polydisperse particle size distribution. Particles with various sizes correspond to different resonance frequencies, which are disadvantageous for uniform and isotropic wave propagation suppression; therefore a larger β leads to a lower TM PBG.

Lastly, the neighbor-neighbor particle distribution is important because optical wave confinement, which is an important property of PBG, is a local effect. For every particle P_0, there are a group of n neighboring particles $(P_1, P_2 \ldots P_n)$ with particle to particle distance $d_{0\langle-\rangle i} < 1.5d_0$. Here $d_{0\langle-\rangle i}$ is the distance between the particle P_0 and the particle P_i, and d_0 is the characteristic length scale defined previously. $1.5d_0$ is selected as the criterion to identify whether two particles are neighbors. The normalized deviation of the particle to neighbor particle distance for particle i is

$$X = \sqrt{\sum_{j=1}^{n_i} (d_{i\langle-\rangle j} - d_0)^2/(n_i - 1)}/d_0. \quad (5)$$

Here, n_i is the number of neighbor particles of particle P_i. We define the third factor, γ, to represent the averaged X for the associated PBG structure

$$\gamma = \sum_{i=0}^{M} \sqrt{\sum_{j=1}^{n_i} (d_{i\langle-\rangle j} - d_0)^2/(n_i - 1)}\,/Md_0. \quad (6)$$

A larger γ indicates a more polydisperse neighbor particle distance distribution and lower local positional order. Loss of short range order is disadvantageous for coherent scattering and the isotropic local confinement of the electromagnetic (EM) wave is hard to achieve due to the leakage from a nonuniform neighbor particle distribution; therefore a large γ leads to lower TM PBG.

According to the above analysis, all three factors bring strong impact on the TM PBG size. We define an overall morphological factor (q) as a linear combination of three geometric factors:

$$\begin{aligned} q &= c_\alpha \sum_{i=1}^{M} \left(\sqrt{\oint_{\partial s} \Delta r_i^2 \, ds}/S_i \bar{r}_i \right)/M \\ &\quad + c_\beta \sqrt{\sum_{i=1}^{M} (A_i - \bar{A})^2/(M-1)}/\bar{A} \\ &\quad + c_\gamma \sum_{i=0}^{M} \sqrt{\sum_{j=1}^{n_i} (d_{i\langle-\rangle j} - d_0)^2/(n_i - 1)}\,/Md_0 \\ &= c_\alpha \alpha + c_\beta \beta + c_\gamma \gamma. \end{aligned} \quad (7)$$

Here, c_α, c_β, and c_γ are positive weighting coefficients for the geometric factors, which are functions of permittivity contrast ratio. Next, we calculate the individual geometric factors of the 17 structures and the associated TM PBGs for three permittivities: i) silicon/air contrast ratio (ε_2:ε_1 = 13:1); (ii) GaAs/air contrast ratio (ε_2:ε_1 = 11.4:1), and (iii) silicon nitride/air contrast ratio (ε_2:ε_1 = 4:1). The size of PBG is determined from the local density of states calculated via finite-difference time-domain (FDTD) method [18,19]. The geometrical parameters of the 17 structures and the associated TM PBGs are shown in supplementary material (supplemental Table 1) [20]. According to the data, we propose a simple linear model to correlate the TM PBG and the overall geometrical factor:

$$\text{PBG size} = \Delta\omega/\omega = b - kq. \quad (8)$$

For ε_2:ε_1 = 13:1, values of $c_\alpha = 0.97$, $c_\beta = 1.03$, and $c_\gamma = 0.5$ lead to the best correlation: the correlation coefficient (R) equals 0.95. The slope (k) in Eq. (8) equals 0.3 and the intercept (b) equals 0.46. For ε_2:ε_1 = 11.4:1, values of $c_\alpha = 0.31$, $c_\beta = 0.64$, and $c_\gamma = 0.5$ lead to the best correlation: $R = 0.94$, $k = 0.58$ and $b = 0.45$. For ε_2:ε_1 = 4:1, values of $c_\alpha = 0.05$, $c_\beta = 0.21$, and $c_\gamma = 0.5$ lead to the best correlation: $R = 0.85$, $k = 0.98$ and $b = 0.246$. From inspection of the weighting coefficients, the most important parameter at high refractive index contrast is the standard deviation of the particle area distribution (β) while the particle distribution factor γ is the most important parameter at low refractive index contrast. The PBGs of the structures are plotted as the black squares in Fig. 2 and the lines in Fig. 2 are the linear models from Eq. (8). For ε_2:ε_1 = 13:1, the TM PBG sizes of the structures deviate less than 3.1% gap size from the linear relation. For ε_2:ε_1 = 11.4:1, the deviation is less than 4.5% gap size. For ε_2:ε_1 = 4:1, the deviation is less than 6.0% gap size. Figure 2 indicates that the overall geometric factor q and the TM PBG size are related as the trend that PBG size decreases with increased q as expected.

In Fig. 2, PCs and PQCs consisting of uniform circular rods (R-p6 mm, 8 mm, 10 mm, and 12 mm) have zero shape anisotropy parameter ($\alpha = 0$) and zero standard deviation of area ($\beta = 0$). Therefore they have low overall factors. Further, circular particles lead to strong isotropic Mie resonance; therefore, they have large PBGs and occupy up left corner of the figure. If $A - \bar{A} \neq 0$, such as occurs for the R-p6mm $- 0.2\Delta A$ structure in Fig. 1(b) and the R-p6mm $- 0.4\Delta A$ structure in Fig. 1(c), the PBG size decreases as the area deviation increases.

Compared to PQCs consisting of rods, PQCs consisting of ovals (O-8 mm, O-10 mm, and O-12 mm) have a higher overall factor q because of the noncircular features. The optical paths along the long axis (nd_{long}) and the short axis (nd_{short}) of the oval feature are different, which leads to an anisotropic resonance condition. Therefore they have smaller TM PBGs and occupy the middle area in Fig. 2.

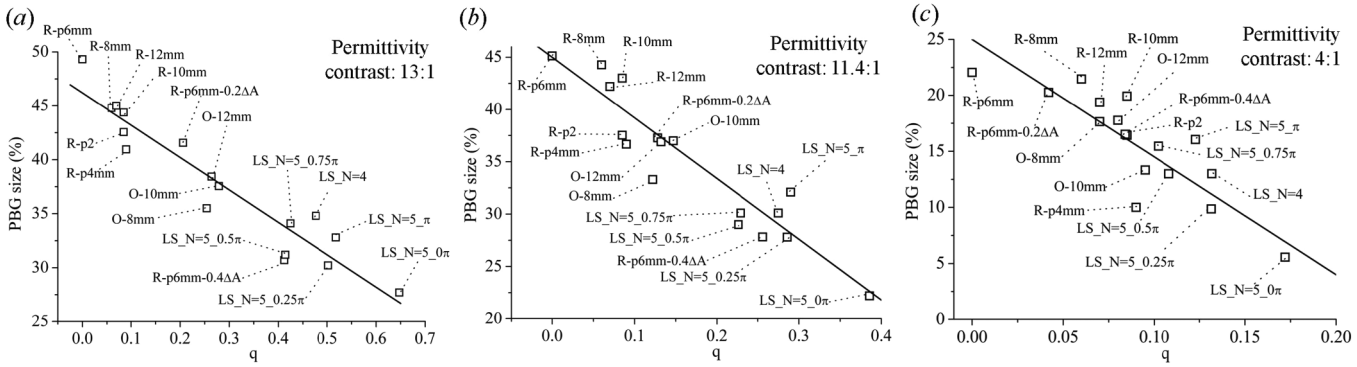

FIG. 2. The relationship between the overall geometric factor q and the size of TM PBG for three permittivity contrasts.

PQCs defined by level set equations, according to Fig. 1(l) through 1(q), have noncircular features ($\alpha > 0$), nonuniform particle area distribution ($\beta > 0$), and nonuniform neighbor particle distance distribution ($\gamma > 0$). This leads to high overall morphological factors and low TM PBGs. Therefore these structures occupy the bottom right corner in Figs. 2(a) and 2(b). As refractive contrast decreases, the PBG sizes of the structures also decrease. PQCs are more robust compared to photonic crystals though they do not exhibit higher PBGs than photonic crystals. For high permittivity contrast, a noticeable case is LS-$N = 5_\varphi = 0\pi$: the particle area distribution is highly polydisperse ($\beta = 0.4$), so the expected lowest TM PBG, which is supposed to be between the first and the second resonance frequencies [12,17], is destroyed by leaky modes and the actual lowest TM PBG for this structure is between the second and the third frequencies. Because of this shift toward higher frequency, the size of TM PBG is relatively lower than other LS-QCs.

In the above discussion, we focused on the lowest PBG, which is usually the largest PBG for 2D photonic crystals. Among the 17 structures investigated, the structure of the triangular lattice (R-$p6$mm) is an interesting photonic crystal device platform due to its large PBG. Next we use geometrical factors to predict the impact of possible experimental errors on the size of TM PBG. For example, we introduce a random deviation of particle area ($A = \bar{A} \pm \delta A$) to the R-$p6$ mm structure with permittivity contrast ε_2:ε_1 = 13:1. The decrease of photonic band gap due to the experimental fabrication error δA can be estimated using the prediction based on the associated geometrical factors and the linear approximation in Eq. (8). For $\delta A = 0.1\bar{A}$, the PBG size is predicted to be 43% and the FDTD simulation indicates that the actual PBG size is 46%. For $\delta A = 0.2\bar{A}$, the PBG size is predicted to be 39.8% and the FDTD simulation indicates that the actual PBG size is 42%. For $\delta A = 0.3\bar{A}$, the PBG size is predicted to be 36.7% and the FDTD simulation indicates that the actual PBG size is 34.6%. Next, we introduce three kinds of perturbations to the R-$p6$ mm structure: in addition to the particle area deviation ($\delta A = 0.2\bar{A}$), every particle has 40% probability to have its center shifted from the original coordinate (x, y) to ($x \pm \delta x$, $y \pm \delta y$); here δx, $\delta y = 0.14 d_0$. Also, we assume the particle shape deforms to be oval with aspect ratio $d_{\text{long}}/d_{\text{short}} = 1.5$ and random orientation. Such a distorted structure has an overall factor (q) of 0.385 and the PBG size is predicted to be 34%. The FDTD simulation indicates that the actual PBG size is 31.9%. All 4 tests above show that the actual PBG sizes deviate from the predictions based on geometrical factors less than 4% PBG size.

Our concept of developing a statistical parameter related to the structural geometry can be extended to 3D although in order to be self supporting, dielectric or air structures need to have the dielectric regions connected. For resonance dominant TM gap formation, a ''tight binding'' structure is necessary, requiring thin connecting ''bonds'' between the larger dielectric nodes. The q factor in 3D will then be related to variations in the shape, sizes and distances of the nodes as well as the overall isotropy of the structure.

In conclusion, we employed a novel statistical procedure to correlate the geometric properties of 17 PBG structures and their TM PBG sizes. Based on our analysis, to achieve a photonic crystal with a large TM PBG, one needs separate circular particles with uniform distribution. The physical meaning of the interesting optimization procedures proposed before [8,9] are revealed: the PBG optimizations, which are done numerically by tuning the coefficients of level set equations [9] or the gradient-based algorithm known as topology optimization [8], are essentially tuning the particle shape to the near-circular shape ($\alpha \approx 0$) and reaching a uniform particle distribution with nearly the same neighbor particle distance ($\beta \approx 0$ and $\gamma \approx 0$).

This research is partially supported by the U.S. Army Research office through the Institute for Soldier Nanotechnologies, under contract W911NF-07-D-0004; the research is also partially supported by NSF, undergrant DMR-0804449.

*Corresponding author.
elt@rice.edu
Present address: Department of Mechanical Engineering & Materials Science, Rice University, P.O. Box 1892, Houston, Texas 77251, USA.

[1] E. Yablonovitch, Phys. Rev. Lett. **58**, 2059 (1987).
[2] J. Ma and M. L. Povinelli, Opt. Express **19**, 10 102 (2011).
[3] Y. Huo *et al.*, Opt. Lett. **36**, 1482 (2011).
[4] H. Noh *et al.*, Appl. Phys. Lett. **98**, 201109 (2011).
[5] J. Ma and M. L. Povinelli, Appl. Phys. Lett. **97**, 151102 (2010).
[6] Y. Kang *et al.*, Nature Mater. **6**, 957 (2007).
[7] S.-C. Cheng, X. Zhu, and S. Yang, Opt. Express **17**, 16 710 (2009).
[8] O. Sigmund and K. Hougaard, Phys. Rev. Lett. **100**, 153904 (2008).
[9] M. C. Rechtsman *et al.*, Phys. Rev. Lett. **101**, 073902 (2008).
[10] C. K. Ullal *et al.*, J. Opt. Soc. Am. A **20**, 948 (2003).
[11] A. Avgeropoulos *et al.*, Macromolecules **30**, 5634 (1997).
[12] C. Rockstuhl, U. Peschel, and F. Lederer, Opt. Lett. **31**, 1741 (2006).
[13] E. Lidorikis *et al.*, Phys. Rev. B **61**, 13 458 (2000).
[14] C. Rockstuhl and F. Lederer, New J. Phys. **8**, 206 (2006).
[15] A. Della Villa *et al.*, Phys. Rev. Lett. **94**, 183903 (2005).
[16] L. N. Shi, X. Y. Jiang, and C. F. Li, J. Phys. Condens. Matter **19**, 176214 (2007).
[17] R. L. Chern and S. D. Chao, Opt. Express **16**, 16600 (2008).
[18] L. Jia, I. Bita, and E. L. Thomas, Phys. Rev. A **84**, 023831 (2011).
[19] L. Jia and E. L. Thomas, Opt. Lett. **36**, 3416 (2011).
[20] See Supplemental Material at http://link.aps.org/supplemental/10.1103/PhysRevLett.107.193901 for details.